Atmospheric pCO_2 and climate during late Eocene (36 ± 5 Ma) on the Indian subcontinent

B. P. Singh[1,*] and Yong Il Lee[2]

[1]Department of Geology, Banaras Hindu University, Varanasi 221 005, India
[2]School of Earth and Environmental Sciences, Seoul National University, Seoul 151-747, Korea

This communication highlights the level of atmospheric CO_2 and the climatic conditions during Eocene (36 ± 5 Ma) based on measurements of stable carbon and oxygen isotopes of late Eocene soil carbonate (calcretes) occurring in the Himalayan foreland basin sequences. The atmospheric pCO_2 is estimated to be about 930 ppm V at high productivity and about 465 ppm V at low productivity. The covariance of $\delta^{18}O$ and $\delta^{13}C$ suggests that the higher atmospheric CO_2 may be responsible for higher temperature. Moderate weathering intensity (CIA value 70–82) of the host mudstones suggests warm climate associated with reasonable wetness that became dry-subtropical, resulting in calcrete development in the northern part of the Indian subcontinent during late Eocene. Wet subtropical climate demonstrates considerable rainfall at this time interval in the region long before the uplift of the Tibetan plateau. Alternatively, it can be suggested that uplift of the Tibetan plateau began much earlier than presently considered.

Keywords: Atmospheric carbon dioxide, Eocene, Himalayan foreland basin, Indian subcontinent, palaeoclimate.

GLOBAL warming resulting from increased CO_2 levels in modern times has heightened interest in the estimation of atmospheric CO_2 from the ancient climates. Geochemical modelling and field observations of modern soils indicate that a relationship exists between the $\delta^{13}C$ of pedogenic carbonate and pCO_2 of the atmosphere, and $\delta^{13}C$ can be used to infer the pCO_2 of the palaeoatmospheres[1]. The estimated CO_2 levels of soil carbonates based on $\delta^{13}C$ and the GEOCARB III model of Berner and Kothavala[2] are not in conformity with each other. Further, atmospheric CO_2 data from continental records are sparse for late Eocene and Oligocene times to verify their consequences for the Eocene warming[1]. Additionally, there are conflicting views regarding the age of initiation/intensification of the monsoon-related rainfall on the Indian subcontinent and the uplift of the Tibetan plateau, which is considered as the major cause of the Asian monsoon initiation.

Climatic and tectonic history of the last ~ 58 m.y. is preserved in the Himalayan foreland basin sequences that contain thick packages of shallow marine (coastal) and continental deposits. This basin in the western part is envisaged as a marine basin from late Palaeocene to middle Eocene (57.9–43.6 Ma) and continental basin in younger times[3]. The continental sedimentation began with the widespread occurrence of red beds in the Himalayan foreland basin that are exposed in the inner belt of the Sub-Himalaya from Pakistan in the west to northwest India in the east (Figure 1 *a*). Details of outcrop belt and sampling locations are shown in Figure 1 *b*. The age of initiation of the continental sedimentation in the Indian part of the Himalayan foreland basin has been assigned as late Eocene (36 ± 5 Ma) based on palaeomagnetic results[4]. Identically, the earliest continental sediments of the Himalayan foreland basin from Pakistan occurring in strike continuity have been assigned the ages between 36 and 40 Ma based on ^{40}Ar–^{39}Ar dating method[5]. The basal red beds contain calcretes as marker horizons within mudstone host (Figure 2). These calcretes are mainly nodular and form over a metre thick profile showing characteristics of Bk horizons. Also, these calcretes possess micromorphological features such as rhizoliths/rhizocretions, fungal filaments and borings, alveolar septal fabric, and micro-nodules (Figure 3). Therefore, essentially these are pedogenic and a fit case for atmospheric CO_2 estimation as suggested by Ekart *et al.*[1], among others.

Nodular calcrete samples were collected from profiles that occur in reasonable thickness (>50 cm thick) and show horizonation. Detailed thin-section study of these samples was carried out and we identified six samples rich in fungal filaments and borings during the course of thin-section study. In all, seventeen samples were selected for stable isotope analysis, including six fungal filament-rich samples. The samples were sawed and polished from one side and the polished slabs were washed with dilute hydrochloric acid during processing. To avoid diagenetic overprinting, only micritic carbonate was drilled with the help of a dentist drill under continuous observation on a stereoscopic microscope and the carbonate powder was acid-digested according to the method suggested by Bemis *et al.*[6]. The liberated CO_2 was analysed for stable isotopes. The isotopic ratios are relative to PDBV standard with reproducibility of ± 0.05‰ for carbon and ± 0.1‰ for oxygen. Average $\delta^{13}C$ value of fungal filaments poor calcrete samples was used for calculating pCO_2 as per equation of Cerling[7]. Additionally, host mudstone samples were analysed for major oxides on an XRF and the chemical index of alteration was calculated from moles of aluminum, calcium, potassium and sodium oxides by the formula of Nesbitt and Young[8].

The carbonate ion is typically inherited from biological respired CO_2 (e.g. organic decomposition and root respiration) rather than carbonate weathering or groundwater CO_2 because the rate of pedogenic carbonate formation is 10^2 to 10^3 times slower than the rate of soil respiration[9]. Also, transfer of carbon from its oxidized form, CO_2 in the atmosphere to the reduced organic forms (carbohy-

*For correspondence. (e-mail: bpsingh_in@yahoo.com)

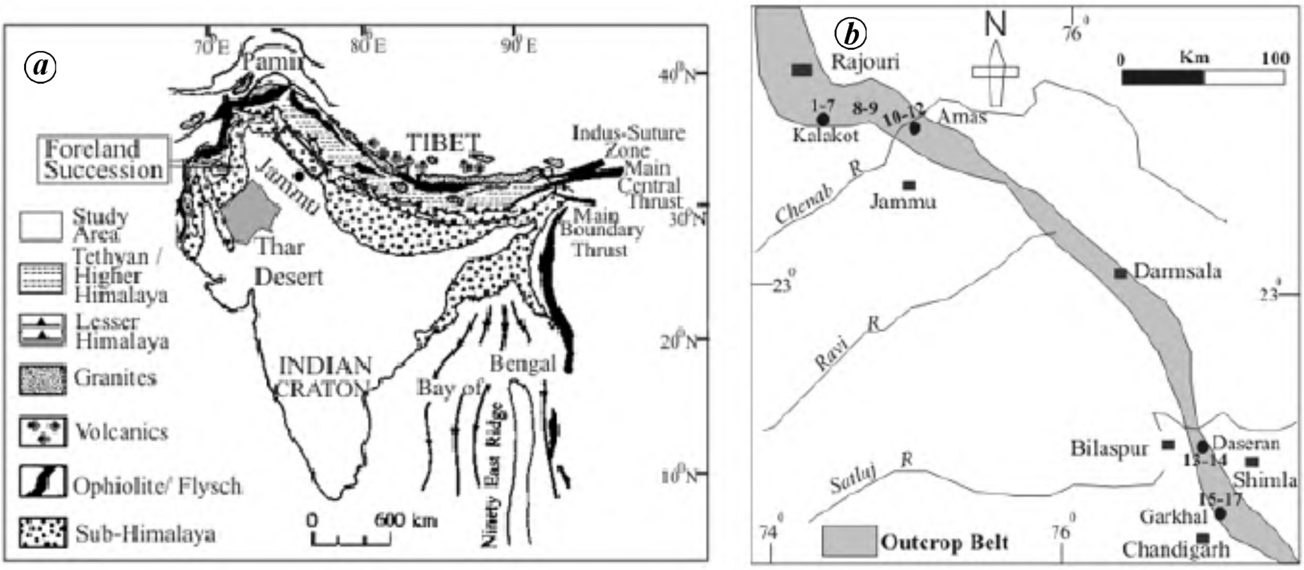

Figure 1. ***a***, Map showing geographical distribution of different tectonic zones of the Himalaya, foreland sequences and the study area (in box) on the Indian subcontinent. Location of Thar Desert is also shown. ***b***, Map showing locations of the calcrete samples (1–17) analysed for stable isotopes in the outcrop belt of the Palaeogene sequences in western Himalaya.

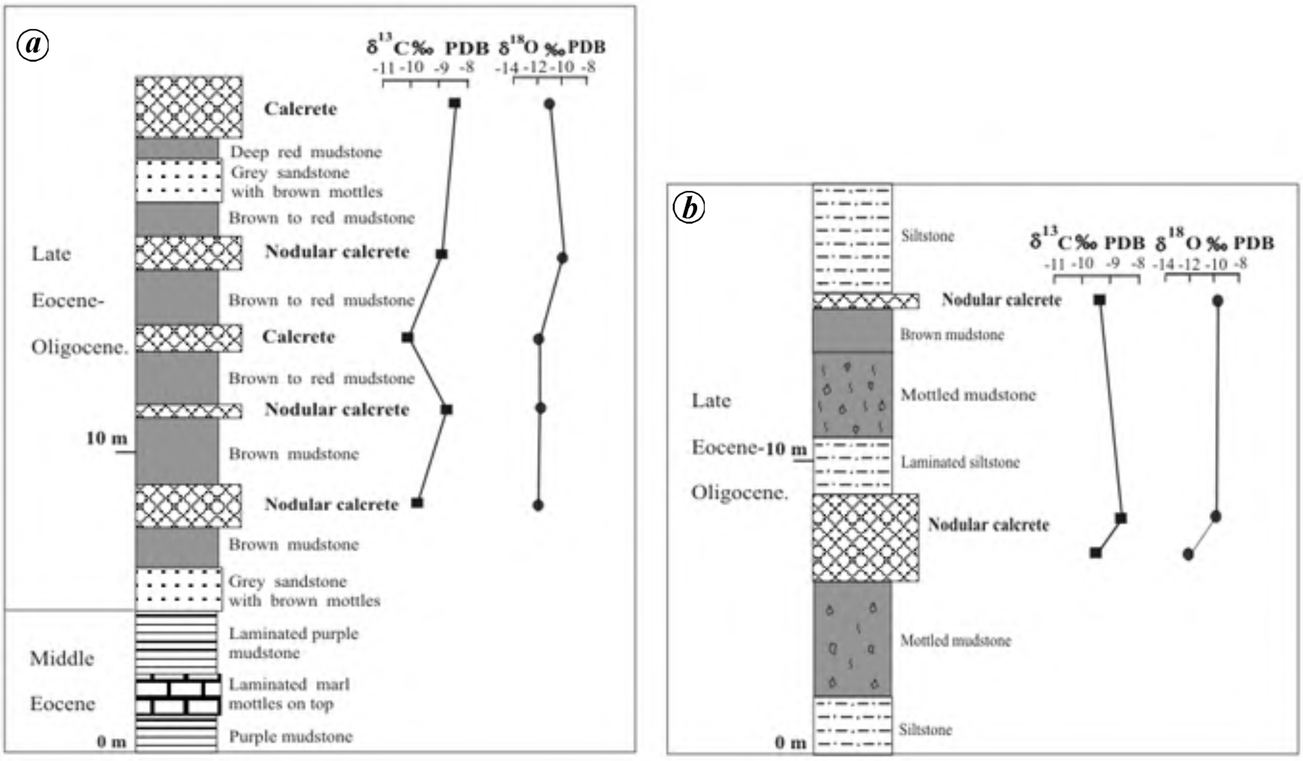

Figure 2. Representative stratigaphic profiles of the late Eocene sequences in the western Himalayan foreland and stable carbon and oxygen isotope variation in the vertical profiles. ***a***, Stratigraphic profile from extreme western end of the study area (Kalakot) shows multiple calcrete horizons and vertical variation of isotopic values. ***b***, Stratigraphic section from extreme east of the studied sections (Garkhal). This section shows two calcrete profiles and variation of stable isotopes from one profile to the other and within a single profile. Note covariance of carbon and oxygen isotope values.

drate) in plants result in photosynthesis[10]. During photosynthesis, when plant stomata are open, CO_2 diffuses inward, and O_2 and H_2O diffuse outward to the atmosphere, returning soil moisture to the atmosphere[11]. Diffusion

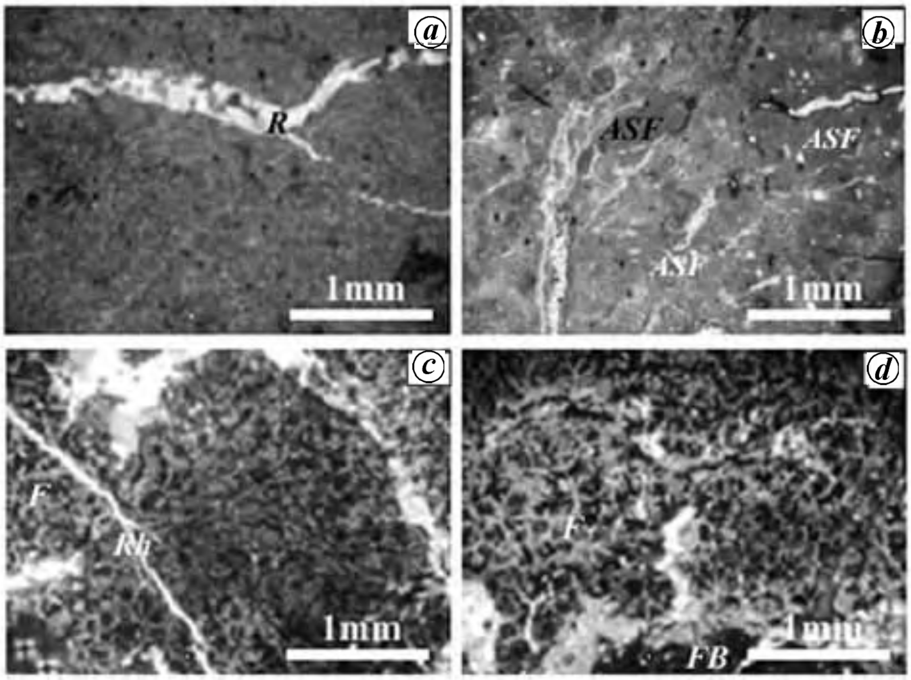

Figure 3. Calcrete photomicrographs. ***a***, Rhizolith (R) showing bifurcation and tapering end. Note sparitic carbonate filling in the root channel and micritic carbonate around it. ***b***, Alveolar septal fabric (ASF) in the calcrete. Note cross-cutting white layers of carbonate in micritic grey matrix. ***c***, Root hair (Rh) and the fungal filament (F) association. Calcification of both root hair and filaments is observed. ***d***, Fungal filaments (F) show a network around fungal borings (FB). Carbonate accumulation can be seen along the filaments.

Table 1. $\delta^{13}C$ and $\delta^{18}O$ values (in ‰) relative to PDB V standard in calcrete samples

Sample nos	$\delta^{13}C_{PDB}V$	$\delta^{18}O_{PDB}V$
1	–9.41	–11.52
2*	–10.12	–13.04
3	–9.81	–11.78
4	–8.75	–11.64
5*	–10.13	–11.83
6	–8.94	–9.77
7*	–8.49	–10.88
8	–8.64	–9.66
9	–9.04	–8.53
10*	–11.23	–11.16
11	–8.85	–9.89
12*	–10.76	–12.52
13	–8.96	–10.39
14*	–10.19	–12.60
15	–9.66	–12.58
16	–8.68	–8.72
17	–9.49	–9.78

*Samples rich in fungal filaments and related features.

of $^{12}CO_2$, a lighter molecule is more rapid in plant tissues than that of $^{13}CO_2$, which composes[10] about 1.1% of atmospheric CO_2. Also inside the leaf, ribulose bisphosphate carboxylase has a higher affinity for $^{12}CO_2$ resulting in more $^{12}CO_2$ to enter into the leaf than $^{13}CO_2$ in a given period of time and as a consequence, the organic matter has very negative $\delta^{13}C$ (–28‰)[10,11].

In the studied calcretes, the $\delta^{13}C$ varies from –8.5 to –11.2‰, whereas $\delta^{18}O$ varies from –8.5 to –13.1‰ (Table 1). Considering calcretes that are poor in fungal filaments and related features, the range of $\delta^{13}C$ value reduces and comes down between –8.8 and –9.8‰ with an average value of –9.2‰. The negative $\delta^{13}C$ and $\delta^{18}O$ values in the studied calcretes demonstrate higher concentrations of lighter isotopes. Also, it is noted that calcretes rich in fungal filaments and associated biogenic features are enriched in lighter stable isotopes and show more negative values (Figure 4 and Table 1). The host mudstones on which calcrete bands have developed are rich in silica and alumina compared to other major oxides and K_2O is more than Na_2O. Chemical index of alteration, an index of weathering intensity, ranges from 70 to 82 (Figure 5).

The atmospheric CO_2 commonly contributes to the soil carbonate and shows less negative $\delta^{13}C$ as compared to the soil organic matter, which also includes carbon from roots respiration and plants decay in addition to atmospheric contribution[7]. Further, mycorrhizal association with roots enhances uptake of many nutrients and increased uptake of phosphorous enhances the rate of photosynthesis, which results in fast fixation of carbon dioxide from the atmosphere by the host plants[12]. On the other hand high soil productivity, inferred from the presence of fungal hyphae, may lead to greater oxidation and respiration of soil material and greater oxidation and respiration may result in more negative soil carbonate $\delta^{13}C$ values[9]. Here, we interpret that the more negative $\delta^{13}C$ values in the calcretes that preserve fungal hyphae are likely attributed to high soil productivity and oxidation of soil organic matter, rather than increased fixation of atmospheric CO_2 in them. Additionally, mycorrhizae provide 100 times more surface area and 10,000 times more length of absorbing organs as a consequence of its 100 times smaller size than the associated root hairs[12]. Therefore, the higher absorbing capacity of the fungal hyphae may be responsible for the lighter $\delta^{18}O$ values in the calcretes rich in them.

Assuming that pedogenic carbonate forms in isotopic equilibrium with soil gas throughout the soil profile, CO_2 palaeobarometer equations of Cerling[7] allows to estimating atmospheric CO_2 from $\delta^{13}C$ of soil carbonates and $\delta^{13}C$ of soil organic matter[1]. The isotopic values for determining pCO_2 in the soil carbonates depend upon types of vegetation using C_3, CAM and C_4 photosynthetic pathways, temperature, soil porosity and depth of soil development and atmospheric pCO_2 can be estimated only in cases of C_3-dominated photosynthesis[7]. The range of $\delta^{13}C$ from –8.5 to –11.2‰ in the present case suggests that the C_3 plants composed of trees, shrubs and some grasses dominated the floral community during late Eocene. Commonly, the carbon isotopic composition of the soil organic matter from C_3-dominated Eocene paleosols is about –24‰[1] and the difference between coexisting soil organic matter and pedogenic carbonate in their carbon isotopic composition is 14–16‰, as a result of equilibrium fractionation between carbon isotope species and the diffusive gases[7]. In the present study, soil organic matter $\delta^{13}C$ value of –24‰ is taken as a reference for the pCO_2 estimation and a difference of 14.9‰ on an average is found between the carbon isotopic composition of the soil organic matter and the soil carbonate.

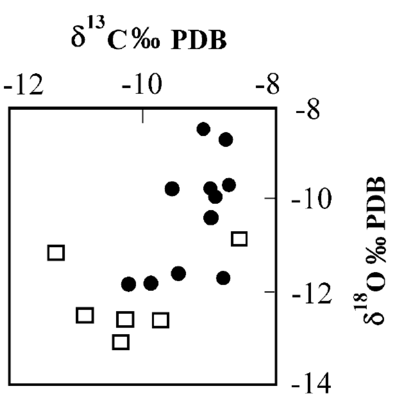

Figure 4. Bivariate plot showing distribution of $\delta^{18}O$ and $\delta^{13}C$ in calcretes of the Himalayan foreland. Values of less mature calcrete are shown with filled circles and calcretes possessing biogenic features with open quadrangle. Both $\delta^{18}O$ and $\delta^{13}C$ show high negative values. $\delta^{18}O$ is higher in the samples in which $\delta^{13}C$ is higher and vice versa with few exceptions.

In the pCO_2 estimation, the soil temperature plays a pivotal role in respiration rate and productivity and the rates of respiration are not exactly known for the geological pasts[1]. As a consequence, soil respired CO_2 equals to 10,000 ppm V with high productivity in warm conditions (temperature = 25°C) and soil respired CO_2 equals to 5000 ppm V with low productivity in cool conditions (temperature = 15°C)[7]. In the present case, the pCO_2 is calculated both at high respiration rate as well as low respiration rate and the average values are 930 and 465 ppm V respectively (Figure 6). Hence, atmospheric pCO_2 is estimated to be a maximum of 930 ppm V during late Eocene (~36 Ma) on the low latitude region of the Indian subcontinent. This value of atmospheric carbon dioxide is much lower than that estimated from 45 Ma soil carbonates of Claron, Utah (1950 ppm V) and even lower than that estimated from 25 Ma Salla (Bolivia) soil carbonates (1470 ppm V) by Ekart *et al.*[1]. The low atmospheric CO_2 demonstrates that there was a period of low atmospheric CO_2 around 36 Ma in between 45 and 25 Ma. This may be true as a result of cyclic variations in the levels of atmospheric carbon dioxide of the geological past.

Pedogenic calcretes form in dry subtropical climatic zones between 10 and 30° latitudes, and the dry subtropical palaeoclimatic zone is characterized by low annual precipitation and seasonal differences in temperature[13]. Palaeomagnetic data[14] indicate that the northern part of the Indian subcontinent was located between 10 and 20°N before 35 Ma. Therefore, the latitudinal position favoured calcrete formation on this part of the continent. Pedogenic calcrete forms by the carbonate accumulation after the end of rainy season (after July–August in the modern Indian summer monsoon) in the Thar Desert and during

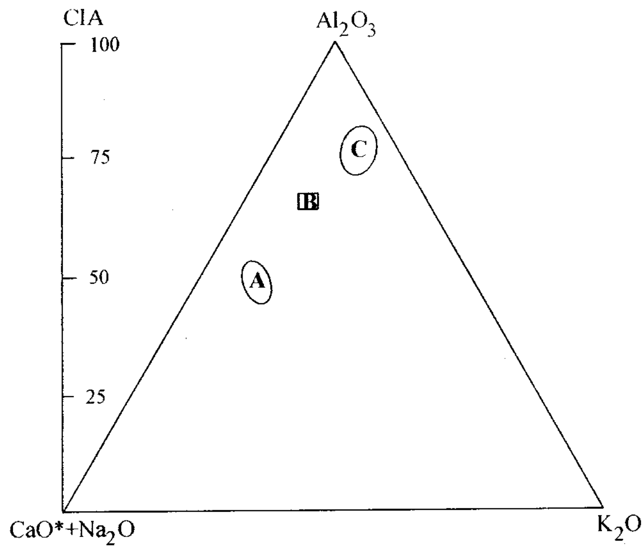

Figure 5. A–CN–K diagram exhibiting relative fields and CIA values of river-suspended sediments from the glaciated terrain (A) (after Singh *et al.*[22]), Ganga River sediment (B) (after McLennan[21]) and late Eocene mudstones of the host calcretes (C).

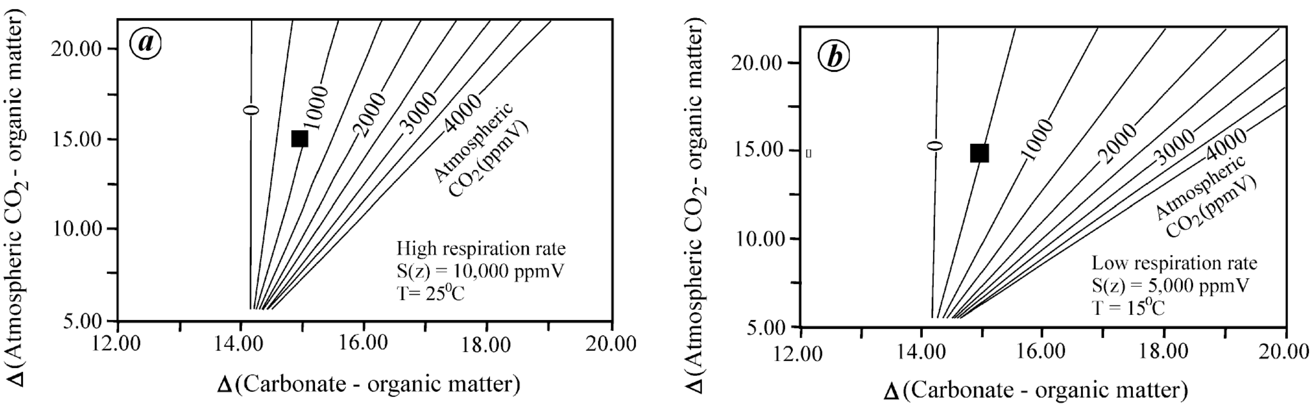

Figure 6. Atmospheric carbon dioxide estimation plots show CO_2 level during late Eocene (filled quadrangle); (after Cerling[7]). ***a***, CO_2 level at high productivity where soil CO_2 (*Sz*) is 10,000 ppm V. ***b***, CO_2 level at low productivity where soil CO_2 (*Sz*) is 5000 ppm V.

the time period of carbonate accumulation (October–March), soil temperatures vary from 22–32°C at a depth of 30–50 cm in the Thar Desert[15,16]. Temperature of carbonate formation, precipitation intensity, source of moisture and shifts in seasonality can be inferred from $\delta^{18}O$ of pedogenic carbonates[17,18]. The range of $\delta^{18}O$ value from –8.5 to –13.1 suggests that the studied calcretes were precipitated under the influence of fresh water after the rainy season. Their precipitation might be associated with high surface temperatures also. Andrews *et al.*[18] found positive correlation between $\delta^{18}O$ and $\delta^{13}C$ and argued that temperature was dependent on level of soil respired CO_2 in Quaternary pedogenic calcretes of the Thar Desert. In the studied calcretes, the covariance of $\delta^{18}O$ and $\delta^{13}C$ suggests that high levels of atmospheric/soil respired CO_2 was, in turn, related to high surface temperature during the precipitation of them. This analogy also exists in the present climatic system where anthropogenic contribution towards increase in atmospheric CO_2 level is resulting global temperature rise. Hence, we predict that higher value of atmospheric CO_2 than the present day value led to elevation in surface temperature during late Eocene times.

Continental sedimentation in the Himalayan foreland basin is correlated with the proto-(Main Central Thrust) formation[19] at about 35 Ma. It may be related to a sea-level change in the late Eocene and/or a warm climatic condition associated with soil formation and low supply of the detritus from the hinterland. Mathur[20] has recorded the dominance of palm and poor occurrence of angiosperms and ferns from the late Eocene succession of the Himalayan foreland basin and suggested an open coastal environment during the late Eocene period. Chemical Index of Alteration (CIA), a measure of weathering intensity, is an important index of climatic conditions around the hinterlands from where the sediments are supplied to the depositional basin. CIA values of about 45–55 indicate virtually no weathering, whereas 100 indicates an intense weathering with complete removal of alkali and alkaline earth metals[21]. CIA in a glaciated river catchment of Himachal Pradesh, which experiences cold climate throughout the year, is reported[22] between 41 and 54 and CIA value of the Ganga River suspended sediment[21] is 66. In Figure 5, the range of CIA in the host mudstones (70–82) is higher than the Ganga River sediment value, the catchment area of which experiences a range of summer temperatures from 30 to 50°C and largely summer monsoon-related rainfall. Therefore, the CIA range of the host mudstones suggests that the weathering was moderate as a result of high temperature and high rainfall during late Eocene. The occurrence of calcretes suggests arid/semi-arid climates during intervening periods when soil carbonates accumulated during low supply of sediment in the Himalayan foreland basin, when the atmospheric CO_2 was less than 930 ppm V.

It is considered that uplift of the Tibetan plateau had significant influence on the Asian monsoon system[23,24] and the uplift of the Tibetan plateau to its present elevation is suggested[25] to have taken place around 15 Ma. Later around 11 Ma, largest change in the planktonic foraminiferal assemblages in the Indian Ocean was linked to closing of Indonesian seaway[26] and this may be related to intensification of the Indian monsoon. Similarly –10‰ $\delta^{18}O$ value of soil carbonates from the Himalayan foreland basin sequences demonstrates Asian monsoon intensification at ~10.5 Ma with a clear onset of another[23,24] monsoon intensification at 6 Ma. Large negative values of $\delta^{18}O$ in the studied calcretes suggest a warm condition during late Eocene times, in conformity with the oceanic record, which demonstrates that the Eocene was warmer than the Palaeocene as well as the younger times. Most modern subtropical climates are seasonal, experiencing monsoon related rainfall. On the Indian subcontinent, the warmer phase was linked with sufficient rainfall contributing moderately weathered denudation products (muddy sediment) to the depositional basin. Therefore, the host mudstones deposited during warm and wet climate phases and the calcretes developed during drier phases. This suggests that substantial rainfall began long before the uplift of the Tibetan plateau. Alternatively, it can be suggested that the Tibetan plateau was uplifted even in late Eocene.

$\delta^{13}C$ values of soil carbonates suggest that the level of atmospheric CO_2 was about 930 ppm V in late Eocene on the Indian subcontinent. The moderate weathering conditions under warm and wet climate during the deposition of host mudstones and intervening drier phases during the development of calcretes demonstrate fluctuations in the climate. Elevated levels of atmospheric CO_2 may be responsible for warmer phase resulting in lighter oxygen isotopes (<–10‰) in the late Eocene calcrete samples. The warm and wet climate during mudstone sedimentation may be related to seasonal climatic conditions that existed even during late Eocene. This also suggests that the Tibetan plateau was uplifted much earlier than the previously inferred times of its uplift.

1. Ekart, D. D., Cerling, T. E., Montanez, I. P. and Tabor, N. J., A 400 million year carbon isotopic record of pedogenic carbonate: Implications for paleoatmospheric carbon dioxide. *Am. J. Sci.*, 1999, **299**, 805–827.
2. Berner, R. A. and Kothavala, Z., GEOCARB III: A revised model of atmospheric CO_2 over Phanerozoic time. *Am. J. Sci.*, 2001, **301**, 182–204.
3. Singh, B. P., Evidence of growth fault and forebuldge in the Late Paleocene (~57.9–54.7 Ma), western Himalayan foreland basin, India. *Earth Planet. Sci. Lett.*, 2003, **216**, 717–724.
4. Klootwijk, C. T., Sharma, M. L., Gergan, J., Shah, S. K. and Gupta, B. K., Rotational overthrusting of the northwestern Himalaya: further palaeomagnetic evidence from the Riasi thrust sheet, Jammu foothills, India. *Earth Planet. Sci. Lett.*, 1986, **80**, 375–393.
5. Najman, Y., Pringle, M., Godin, L. and Oliver, G., Dating of the oldest continental sediments from the Himalayan foreland basin. *Nature*, 2001, **410**, 194–197.
6. Bemis, B. E., Spero, H. J., Bijima, J. and Lea, D. W., Reevaluation of the oxygen isotopic composition of planktonic foraminifera; experimental results and revised paleotemperature equations. *Paleoceanography*, 1998, **13**, 150–160.
7. Cerling, T. E., Use of carbon isotopes in paleosols as an indicator of the PCO_2 of the paleoatmosphere. *Global Biogeochem. Cycle*, 1992, **6**, 307–314.
8. Nesbitt, H. W. and Young, G. M., Early Proterozoic climates and plate motions inferred from major elements chemistry of lutites. *Nature*, 1982, **299**, 715–717.
9. Cerling, T. E., The stable isotopic composition of modern soil carbonate and its relationship to climate. *Earth Planet. Sci. Lett.*, 1984, **71**, 229–240.
10. Schlesinger, W. H., *Biogeochemistry: An Analysis of Global Change*, Academic Press, California, USA, 1997, p. 588.
11. O'Leary, M. H., Carbon isotopes in photosynthesis. *Bioscience*, 1988, **38**, 328–336.
12. Fitter, A. H., Costs and benefits of mycorrhizal infection. *Experientia*, 1991, **47**, 350–355.
13. Mack, G. H. and James, W. C., Paleoclimate and the global distribution of paleosols. *J. Geol.*, 1994, **102**, 360–366.
14. Klootwijk, C. T., Gee, J. S., Peirce, J. W., Smith, G. M. and McFadden, P. L., An early India-Asia contact: Paleomagnetic constraints from Ninetyeast Ridge, ODP Leg 121. *Geology*, 1992, **20**, 395–398.
15. Courty, M. A., Dhir, R. P. and Raghavan, H., Microfabrics of calcium carbonate accumulations in arid soils of western India. In *Micromorphologie des Sols* (eds Fedoroff, M. and Courty, M. A.), Association. Francaise pour 1'Etude du Sols, 1987, pp. 227–234.
16. Gupta, J. P., Some studies on hydrothermal regime and daytime heat fluxes in a desert sandy soil with and without vegetation. *Arch. Meteorol. Geophys. Bioclimate. Ser. B*, 1983, **32**, 99–107.
17. Stern, A. L., Chamberlain, R. C., Reylonds, C. R. and Johnson, D. J., Oxygen isotope evidence of climate change from pedogenic clay minerals in the Himalayan molasses. *Geochim. Cosmochim. Acta*, 1997, **61**, 731–744.
18. Andrews, J. E., Singhvi, A. K., Kailath, A. J., Kuhn, R., Dennis, P. F., Tandon, S. K., and Dhir, R. P., Do stable isotope data from calcrete record late Pleistocene monsoonal climate variation in the Thar Desert of India? *Quat. Res.*, 1998, **50**, 240–251.
19. Le Fort, P., Evolution of the Himalaya, In *The Tectonic Evolution of Asia*. (eds Yin, A. and Harrison, M.), Cambridge University Press, 1996, pp. 95–109.
20. Mathur, Y. K., Cenozoic palynofossils, vegetation, ecology and climate of the north and northwestern Sub-Himalayan region. In *The Evolution of the East Asian Environment* (ed. Whyte, R. O.), Center of Asian Studies, University of Hong Kong, 1984, pp. 504–551.
21. McLennan, S. M., Weathering and global denudation. *J. Geol.* 1993, **101**, 295–303.
22. Singh, B. P., Kumar, R. and Kalsotra, B. L., Suspended and dissolved flux in the Baspa River, Kinnaur district, Himachal Pradesh: Evaluation of weathering and erosion. *Geol. Surv. India Spl. Pub*., 2001, **65**, 31–35.
23. Dettman, D. L., Kohn, M. J., Quade, J., Ryerson, F. J., Ojha, T. P., and Himidullah, S., Seasonal stable isotope evidence for a strong Asian monsoon through out the past 10.7 m. y. *Geology*, 2001, **29**, 31–34.
24. Sanyal, P., Bhattacharya, S. K., Kumar, R., Ghosh, S. K. and Sangode, S. J., Mio-Pliocene monsoonal record from Himalayan foreland basin (Indian Siwalik) and its relation to vegetational change. *Palaaeogeogr. Palaaeoclimatol. Palaaeoecol.,* 2004, **205**, 23–41.
25. Spicer, A. R., Harris, B. W. N., Widdowson, M., Herman, B. A., Guo, S., Valdes, J. P., Wolfe, A. J. and Kelley, P. S., Constant elevation of southern Tibet over the past 15 million years. *Nature*, 2003, **421**, 622–624.
26. Srinivasan, M. S. and Singh, A. D., Planktonic foraminiferal evidence for the Neogene paleocenographic changes in the Indian Ocean. Ann. Tech. Meet. IGCP-246 Spec. Publ., Chiang Mai Univ., vol. 9, pp. 179–205.

ACKNOWLEDGEMENTS. B.P.S. thanks to the Department of Science and Technology, New Delhi for a research project on the Palaeogene palaeosols of the Himalaya and J. S. Pawar, R. S. Charak and Dr S. P. Singh for help during field work. He also thanks to the Indian National Science Academy, New Delhi and Korea Science and Engineering Foundation for a fellowship to visit Seoul National University, Korea. This study was also supported by KOSEF (2000-2-13100-003-5 to YIL). Mr Y. W. Lee is thanked for help in sample preparation. The stable isotope measurements and XRF analyses were carried out at the Korea Basic Science Institute. Thanks are due to Prof. A. D. Singh for reading the manuscript.

Received 20 January 2006; revised accepted 18 August 2006